Effects of Adverse Pressure Gradients on the Nature and Length of Boundary Layer Transition

G. J. Walker
University of Tasmania,
Hobart, Australia

J. P. Gostelow
University of Technology,
Sydney, Australia

Existing transition models are surveyed and deficiencies in previous predictions, which seriously overestimate transition length under an adverse pressure gradient, are discussed. A new model for transition in an adverse pressure gradient situation is proposed and experimental results are provided that confirm its validity. A correlation for transition length is advanced that incorporates both Reynolds number and pressure gradient effects. Under low free-stream turbulence conditions the basic mechanism of transition is laminar instability. There are, however, physical differences between zero and adverse pressure gradients. In the former case, transition occurs randomly, due to the breakdown of laminar instability waves in sets. For an adverse pressure gradient, the Tollmien–Schlichting waves appear more regularly with a well-defined spectral peak. As the adverse pressure gradient is increased from zero to the separation value the flow evolves continuously from random to periodic behavior and the dimensionless transition length progressively decreases.

Introduction

Turbomachinery designers have become reliant on advanced computational methods to predict flows over blading. An essential requirement of these codes is their ability to predict the state of the boundary layer on the blade surface. Difficulties have often been encountered due to inadequacies in existing boundary layer transition prediction procedures. It has been necessary to resort to crude, and often unrealistic, assumptions for the codes to run. This is especially so of the adverse (or positive) pressure gradient regimes encountered by compressor blading. The problems arise because the existing experimental transition data for adverse pressure gradient flows are inadequate.

Transition on the blades of axial turbomachines may eventuate from a variety of causes including two-dimensional viscous instability, centrifugal instability on concave surfaces, surface roughness, and the diffusion of free-stream turbulence into the boundary layer. Laminar instability processes can be significantly influenced by external disturbances such as acoustic forcing, wake passing and free-stream turbulence fluctuations.

The basic mechanism may be considered to be laminar instability, which is, however, subject to being "bypassed" and therefore masked by turbulence and other effects. For this reason a series of experiments was undertaken in a relatively clean flow environment to elucidate the influence of pressure gradient on laminar instability processes before addressing other real-flow attributes of turbomachines, such as free-stream turbulence.

The present investigation is concerned with the physics of transition under adverse pressure gradients and in the absence of interference from bypass mechanisms. The emphasis is on differences in transition modes between flows with and without an adverse streamwise pressure gradient. A new model for transition under these conditions is proposed and experimental results are presented in an attempt to validate the model.

One result of this work is a new correlation for transition length, which is broadly supported by the limited data available. The new model and correlation differ substantially from existing procedures. They offer a basis for more accurate transition modeling, which should be capable of describing laminar separation effects and can be extended to other influences on transition, such as free-stream turbulence effects.

Transition Resulting From Two-Dimensional Viscous Instability

Transition arising from two-dimensional viscous instability was the dominant mechanism leading to the onset of turbulence in the present investigation. The sequence of events involved in this type of transition is as follows:

(a) Instability to Two-Dimensional Disturbances. Above a critical Reynolds number, the laminar boundary layer becomes unstable to two-dimensional disturbances. Subsequent ampli-

Contributed by the International Gas Turbine Institute and presented at the 34th International Gas Turbine and Aeroengine Congress and Exhibition, Toronto, Ontario, Canada, June 4–8, 1989. Manuscript received at ASME Headquarters February 1, 1989. Paper No. 89-GT-274.

fication leads to the formation of Tollmien-Schlichting (T-S) waves.The onset of instability and the initial growth of T-S waves are well described by linearized theory and solutions to the resulting Orr-Sommerfeld equation. The shape of the neutral stability curve depends on the laminar velocity profile, which is determined principally by the streamwise pressure gradient. The range of frequencies receiving amplification varies with the boundary layer Reynolds number.

(*b*) Three-Dimensional Instability and Nonlinear Amplification. After sufficient amplification of the two-dimensional disturbances, a regular spanwise flow distortion becomes apparent. This three-dimensionality introduces streamwise vorticity and causes a rapid nonlinear amplification of the spanwise waves into vortex loops (also referred to as vortex trusses, hairpin eddies and lambda vortices). The vortex loops may be arranged either in streamwise rows or in a staggered ("thatched") pattern as shown in Fig. 1. The staggered pattern repeats itself at streamwise intervals of 2 Λ_x, where Λ_x is the wavelength of the primary instability wave, and thus introduces subharmonics at half the T-S wave frequency.

Saric and Thomas (1983) identified two types of staggered pattern having characteristically different ratios of spanwise to streamwise wavelength, Λ_z/Λ_x. The type of three-dimensionality observed was found to depend on the amplitude of the primary disturbance. For disturbance levels less than $0.002U$ at Branch II (the upper branch) of the neutral stability curve, the two-dimensional disturbances decayed without any three-dimensionality appearing. At amplitudes around $0.003U$, a *C*-type system of staggered vortices with Λ_z/Λ_x about 1.5 was obtained. This system, which was investigated theoretically by Craik (1971), is produced by resonant interactions among a triad of one normal and two oblique T-S waves. At amplitudes between 0.003 and $0.006U$, an *H*-type staggered system having a Λ_z/Λ_x of about 0.7 was observed. The latter pattern is explained by instability to three-dimensional disturbances of a basic state comprising laminar flow and a two-dimensional T-S disturbance as described by Herbert (1983).

For amplitudes greater than $0.006U$, Saric and Thomas (1983) observed a *K*-type array of vortices aligned in streamwise rows having a Λ_z/Λ_x of about 0.5. This is the pattern that was observed in the early studies of three-dimensional instability carried out by Klebanoff et al. (1962). More recent experimental studies of events in the nonlinear region have been reported by Kegelman and Mueller (1986).

(c) Breakdown. The initiation of turbulent spots (or "breakdown") occurs through the appearance of high-frequency fluctuations near the heads of the vortex loops. The influence of streamwise pressure gradient on this process has been investigated by Knapp and Roache (1968) and by Arnal et al. (1979a, 1979b).

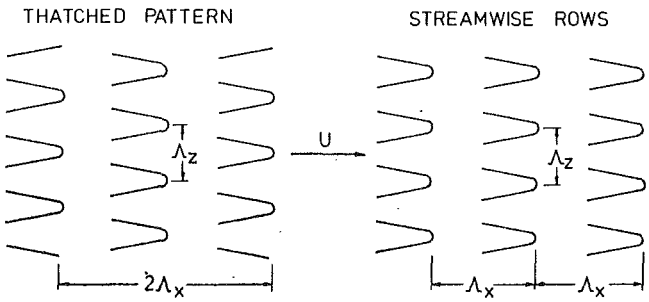

Fig. 1 Vortex loop patterns prior to breakdown

Knapp and Roache found natural transition in zero pressure gradient flows to be characterized by the breakdown of laminar instability waves in sets. These sets translated several wavelengths of the basic T-S wave during amplification, distortion and breakdown. They were interspersed by a significant laminar region following breakdown. The vortex loops resulting from the breakdown of wave sets were usually arranged in a staggered pattern. The "intermittency" frequency with which wave sets appeared was about one tenth of the basic T-S wave frequency.

For natural transition in an adverse pressure gradient, Knapp and Roache observed similar behavior, except that the phenomena became more exaggerated. The formation of wave sets occurred at a higher frequency, and transition approached a continuous process with much shorter intervals between the breakdown of sets. In the nonlinear region, the tendency for vortex loops to be staggered was reduced and a greater proportion appeared in streamwise rows. The work of Arnal et al. (1979b) supports the observation of the more continuous transition process, intermittency becoming more difficult to determine in these circumstances.

In forced transition produced by the introduction of sound waves, with frequencies close to those of the naturally occurring T-S waves, Knapp and Roache found the frequency of all wave regions became locked in to the sound frequency. There was a continuous breakdown of individual instability waves and the vortex loops tended to appear in rows for both zero and adverse pressure gradients.

(d) Merging of Turbulent Spots. The final stage of tran-

Nomenclature

C_p = static pressure coefficient
c_f = skin-friction coefficient
H = form factor = δ^*/θ
L_T = transition length $=(x_T - x_t)$
N = nondimensional spot formation rate $= n\sigma\theta_i^3/\nu$
n = spot formation rate
R_t = transition inception Reynolds number
R_x = length Reynolds number
R_{δ^*} = displacement thickness Reynolds number
R_θ = momentum thickness Reynolds number
T = turbulence level, percent
t = time
U = free-stream velocity
u = local velocity
x = streamwise distance from leading edge
y = normal distance from wall
δ = absolute thickness
δ^* = displacement thickness
γ = intermittency factor
η = dimensionless distance $=(x-x_S)/(x_T-x_S)$
θ = momentum thickness
λ = distance from 0.25 to 0.75 intermittency
λ_θ = pressure gradient parameter $= (\theta^2/\nu)\cdot(dU/dx)$
ν = kinematic viscosity
ξ = dimensionless distance $=(x-x_t)/\lambda$
σ = turbulent spot-dependence area parameter
ρ = density
ω = circular frequency, rad/s
Λ = instability wavelength

Subscripts

S = start of transition ($\gamma = 0.01$)
T = end of transition ($\gamma = 0.99$)
t = start of transition (Narasimha method)
x = streamwise component
z = spanwise component

sition involves a zone of intermittently turbulent flow in which adjacent turbulent spots merge through both streamwise and lateral spreading to form a continuously turbulent flow. Numerous studies of turbulent spot spreading have been reported since the earliest investigation by Schubauer and Klebanoff (1956) of an isolated spot developing in zero pressure gradient.

An isolated spot resembles a downstream-pointing arrowhead in planform. Schubauer and Klebanoff found the growth envelope to approximate a wedge of 22 deg included angle. The convection rates of the spot leading and trailing edges were $0.88U$ and $0.5U$, respectively. These values can be taken as typical, although they are known to vary slightly with Reynolds number and pressure gradient.

Transitional Flow Length

Zero Pressure Gradient. Experimental work by Narasimha and others for constant pressure boundary layers has indicated a universal distribution of turbulent intermittency regardless of the agency causing transition. This distribution is described by

$$\gamma = 1 - \exp[-0.412\ \xi^2]. \tag{1}$$

Narasimha (1957) showed that this result could be derived from the turbulent spot theory of Emmons (1951) on the assumption that spots form randomly in time and cross-stream position at a preferred streamwise location lying close to the upstream end of the transition region x_t. The development of this model is described in a recent comprehensive review of transitional flow behavior by Narasimha (1985).

It also is useful to have an overall measure of transitional flow length. Defining the downstream limit of the transition zone to be the 99 percent intermittency location, the foregoing intermittency distribution gives

$$L_T = (x_T - x_t) = 3.36\lambda. \tag{2}$$

Empirical correlations for the length of the transition zone in constant pressure flows have been given by various workers in the form

$$R_\lambda = A\ R_t^B \qquad (A, B \text{ const}). \tag{3}$$

Dhawan and Narasimha (1958) originally proposed

$$R_\lambda = 5\ R_t^{0.8} \tag{4}$$

as an average fit to their available data, which showed a considerable amount of scatter. Narasimha (1978) later revised this correlation to give

$$R_\lambda = 9\ R_t^{0.75} \tag{5}$$

which is still consistent with the Dhawan and Narasimha data and implies a turbulent spot breakdown rate dependent on local boundary layer thickness.

Arbitrary Pressure Gradient. Chen and Thyson (1971) modeled the transition zone for flows in a pressure gradient by assuming that:

(*i*) Spot propagation velocities at any given station are proportional to the local external velocity $U(x)$;

(*ii*) The spot grows at a constant angle to the local external streamline; and

(*iii*) the hypothesis of concentrated breakdown at x_t remains valid.

In accordance with this model Cebeci and Smith (1974) proposed the intermittency distribution

$$\gamma = 1 - \exp[-G(x - x_t) \int_{x_t}^{x} dx/U] \tag{6}$$

where

$$G = (1/1200) \cdot (U^3/\nu^2)\ R_t^{-1.34}. \tag{7}$$

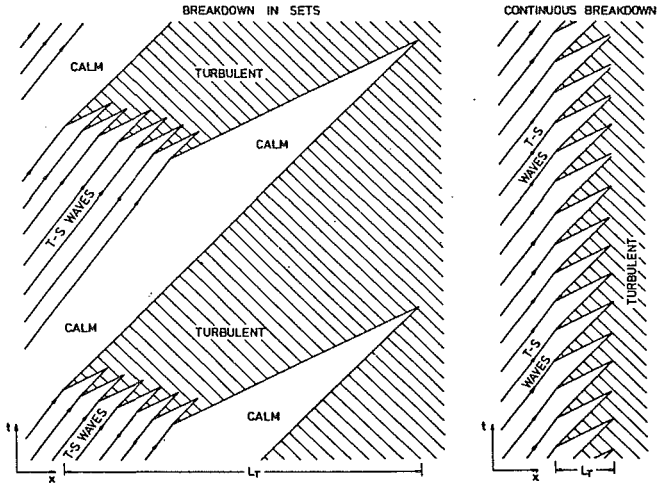

Fig. 2 Time-space distributions of the transition process

The Chen-Thyson model only allows for the effect of pressure gradient on local spot convection velocities and does not encompass any influence of pressure gradient on the mechanics of breakdown. For the case of zero pressure gradient, equations (6) and (7) lead to

$$R_\lambda = 22\ R_t^{0.67} \tag{8}$$

which gives similar results to equation (4) due to compensating variations in the constants used. The model has essentially been calibrated against constant pressure flow data.

Minimum Transition Length. Difficulties experienced by users of computational routines in calculating the boundary layer development on the suction surface of airfoils operating at low Reynolds number have drawn attention to the inadequacies of approaches such as the Chen-Thyson model for the case of a strong adverse pressure gradient. A recent example is given in the computations of Subroto (1987) using the Cebeci-Smith (1974) formulation. On the suction surface of airfoils and compressor blades transition is much more rapid than in constant pressure flows and equations (6) and (7) seriously overpredict the transition length. This can lead to failure of low Reynolds number calculations due to the bursting of laminar separation bubbles in the computed flow (Walker et al., 1988).

These problems can be explained in terms of the influence of pressure gradient on the breakdown mechanism, which was not taken into account in the Chen-Thyson model. The effect of pressure gradient is illustrated by Fig. 2, which shows time-space distributions of laminar and turbulent flow through transition for two characteristically different breakdown mechanisms. The diagrams have been constructed using typical values of U, $U/2$, $U/3$, respectively, for the leading and trailing edge spot convection rates and the T-S wave velocity. The breakdown of instability waves in sets, with an intervening calming period, is seen to produce transitional flow lengths several times greater than in a forced transition situation, where breakdown occurs continuously every cycle of the basic T-S wave. Following Knapp and Roache, transition inception in a strong adverse pressure gradient is expected to result from behavior of the continuous breakdown kind; for constant pressure flows, on the other hand, transition inception is expected to result from breakdown in sets.

In an attempt to estimate the transition length in strongly decelerating flow and to place limits on the possible range of transitional flow lengths, Walker (1987) developed a minimum transition length model based on the continuous breakdown hypothesis. An equispaced spanwise array of turbulent spots was assumed to originate from x_t once each cycle of the basic

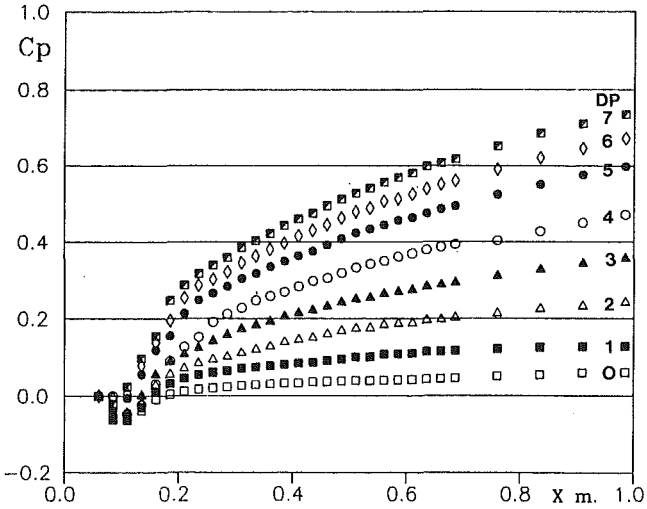

Fig. 3 Streamwise static pressure distributions for different levels of adverse pressure gradient

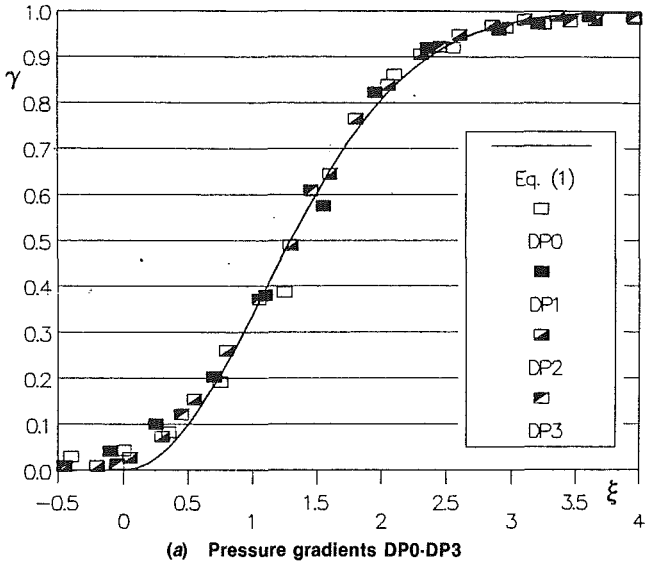

(a) **Pressure gradients DP0-DP3**

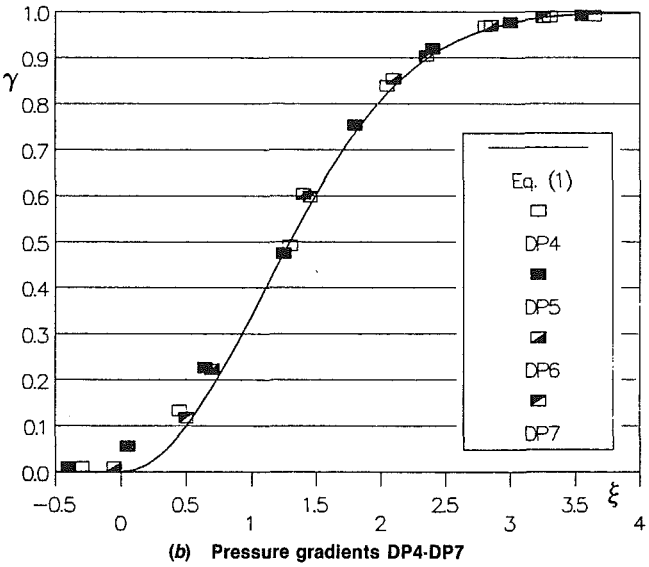

(b) **Pressure gradients DP4-DP7**

Fig. 4 Intermittency distributions for the range of pressure gradients, plotted on a similarity basis

T-S wave. McCormick's (1968) model of an idealized triangular spot spreading at the convection velocities observed by Schubauer and Klebanoff (1956) was then applied to determine the streamwise distance required for adjacent spots to touch through either lateral or longitudinal spreading.

From the stability characteristics of Falkner-Skan boundary layers calculated by Obremski et al. (1969), the locus of maximum disturbance amplification *rate* was correlated by

$$(\omega\nu/U^2) = 3.2\ R_{\delta^*}{}^{-3/2}. \tag{9}$$

This was assumed to approximate the dimensionless frequency of disturbances having the maximum amplification *ratio*. Adopting this frequency for the spot inception rate, and assuming a spanwise spot spacing equal to the basic T-S wavelength, the streamwise spreading was found to be the limiting factor in determining minimum transition length. The corresponding transition length was given by

$$R_{L_T} = 2.3\ R_{\delta^*{}_t}{}^{3/2} \tag{10}$$

which for zero pressure gradient flow, can be written as

$$R_{L_T} = 5.2\ R_t{}^{3/4}. \tag{11}$$

This shows the same functional dependence on Reynolds number as Narasimha's (1978) correlation, equation (7), and also gives a reasonable estimate of transition length for a forced transition case reported by Schubauer and Skramstad (1948).

An Arbitrary Pressure Gradient Transition Model. In arbitrary pressure gradient situations with low free-stream disturbance levels, the transitional flow length might be expected to vary between values predicted by zero pressure gradient correlations and those obtained from the minimum length model just outlined. This will be due to a number of pressure gradient related factors such as turbulent breakdown mechanisms and spot spreading rates. It therefore seems reasonable to attempt a correlation of the ratio of actual transition length to that given by the aforementioned minimum length model in terms of some suitable pressure gradient parameter.

This possibility will be explored in the following discussion using data of the present investigators and other workers. Besides providing further information about the influence of pressure gradient on transition, the analysis will assist in calibrating the minimum transition length model itself.

Experimental Results and Data Analysis

Experimental investigations were undertaken in the low-speed wind tunnel described by Gostelow and Blunden (1988). The previous investigations were undertaken with turbulence grids present upstream of the working section, giving free-stream turbulence levels between 1 and 5 percent. For the subject experiments no such grid was present and the average free-stream turbulence level at inlet was 0.3 percent. Intermittency measurements were made using a single hot-wire probe and a DISA constant temperature anemometer. For most boundary layer velocity traverses, a flattened head pitot tube was used.

Adverse pressure gradients, of varying strength, were imposed by a fairing mounted above the flat plate. This could be rotated incrementally about an axis located 20 mm upstream of the leading edge of the flat plate. Static pressure gradients in a streamwise direction could be measured using both centerline pressure taps and velocity measurements in the free stream. Figure 3 presents the streamwise distributions of static pressure, measured using the static taps, for the different fairing settings used. There was no evidence of separation from the fairing in the region of interest. The pressure gradients were designated DP0-DP7, commencing with zero and in increasing order of adverse pressure gradient.

Intermittency values were determined on-line using a meter developed by Alt (1987). With this meter, sampling times up

to 100 s were possible. The setting of threshold levels needed particular attention for these measurements, especially under strong adverse pressure gradients where strong periodic signals were observed both before and after turbulent breakdown.

The intermittency distributions obtained for the various pressure gradients are presented in Fig. 4. These are presented in the similarity form advocated by Narasimha (1957). All intermittency data were plotted in terms of the variable

$$F(\gamma) = [-\ln(1-\gamma)]^{1/2} \tag{12}$$

and from the resulting plots the effective transition inception x_t, obtained by linear extrapolation to the η-axis, and effective transition length, λ, were determined. The rescaled intermittency distributions were then plotted in comparison with Narasimha's universal intermittency function given in equation (1).

Agreement with the universal function is seen to be reasonable. The Narasimha procedure clearly provides a viable basis for representation of the transition region. Although data were obtained for a range of intermittencies, including 1 percent as a notional transition inception value, data consistency is maximized by designation of the "t" intercept as the start of transition.

Boundary layer velocity profiles were derived in the form of dimensionless velocity as a function of dimensionless traverse height. The form of these was generally in accordance with the plots of Gostelow and Blunden although full traverses were carried out for fewer intermittency values than in the previous study.

The resulting velocity distributions were integrated to provide integral parameters at the start and end of transition and for some intermediate locations. The results for R_x and also for R_θ appear in Fig. 5; the values for both transition inception and completion are plotted against $\lambda_{\theta t}$ in this figure.

The general shape of the R_x and R_θ plots is in accordance with the results presented in Gostelow and Blunden for a 1.7 percent turbulence level. Transition inception occurs at a value of $R_{\theta t}$ that declines mildly with increasing adverse pressure gradient. This decline levels off to a fairly constant value of $R_{\theta t}$ under moderately strong adverse pressure gradients. The completion of transition, on the other hand, occurs very much sooner as an increasingly adverse pressure gradient is imposed. As with the previous results, the tendency for the transition zone to become shorter is strong and consistent. The change is most marked when a zero pressure gradient is replaced by even a weak adverse one.

The data for the various adverse pressure gradient conditions have been analyzed according to the procedure of Narasimha (1985). A value of dimensionless turbulent spot formation parameter, N, has been obtained for each pressure gradient and these also are plotted as a function of $\lambda_{\theta t}$ in Fig. 5. Although the derivation of N depends upon a number of assumptions the value for zero pressure gradient is broadly in accordance with the compilation of Narasimha (1985). The trend reflects the rapidly decreasing transition length as the pressure gradient parameter becomes more adverse, N varying inversely as the square of transition length.

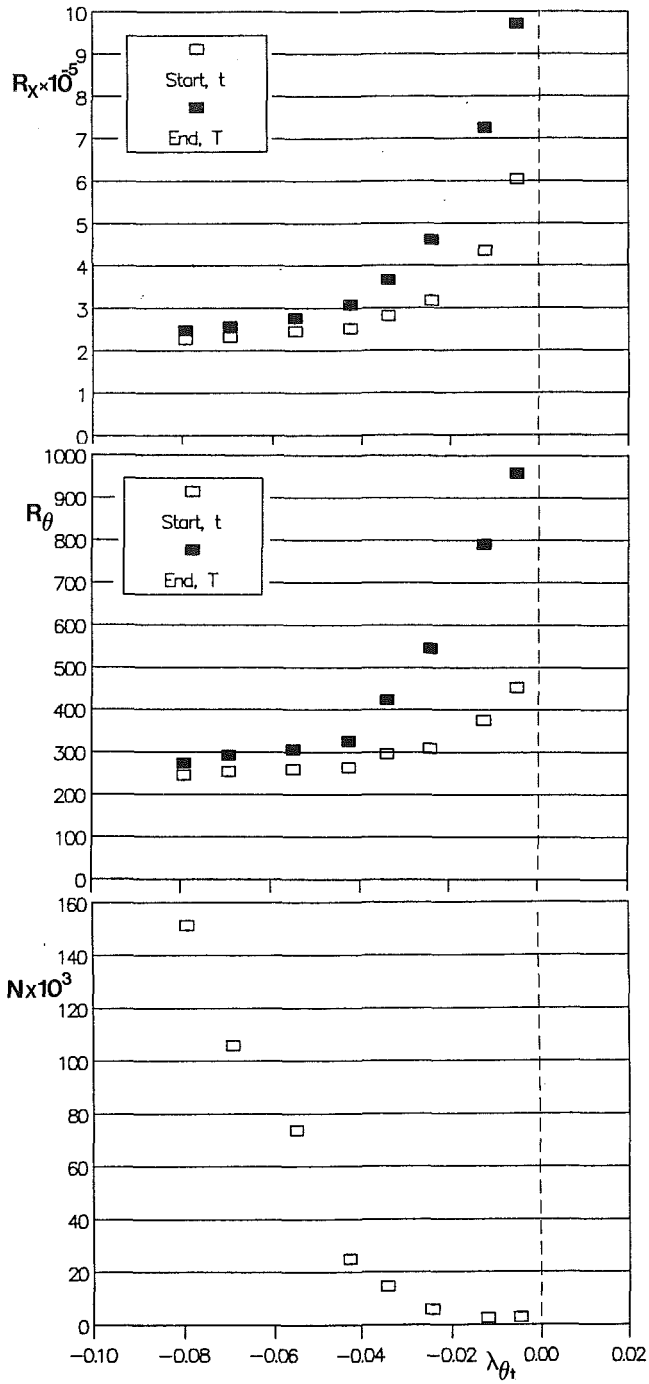

Fig. 5 Variation of R_x, R_θ and spot formation rate parameter, N, with pressure gradient parameter

Hot-Wire Anemometer Signals. A principal reason for the shorter transition lengths and strong increases in turbulent spot formation rates is the different physical nature of the flow under an adverse pressure gradient. Anemometer traces have been presented in Fig. 6 that represent some of the more identifiable events. Traces have been given for the zero pressure gradient case and for cases representing $\lambda_{\theta t}$ values of -0.034 and -0.069; for each pressure gradient intermittency values of 10, 50 and 90 percent have been represented. The traces have identical frequency and amplitude scales and were printed from a Hewlett-Packard 5420A Digital Signal Analyzer set to a bandwidth of 3.2 kHz and digitizing to 512 points. While these limitations have resulted in the loss of some high-frequency detail in the turbulent spot regions, the traces nevertheless represent the principal features of the flow.

The zero pressure gradient traces show clear evidence of T-S waves breaking down in sets with intervening calming periods. The turbulent spots are well defined making the measurement of intermittency a relatively easy task. While the intervals between spots are largely devoid of instability waves, it is nevertheless possible to discern some wave amplification and breakdown occurring at all stages of transition.

The medium pressure gradient traces still show evidence of the development of wave sets, but some T-S wave activity of lower amplitude can now be seen over most of the intervals between sets.

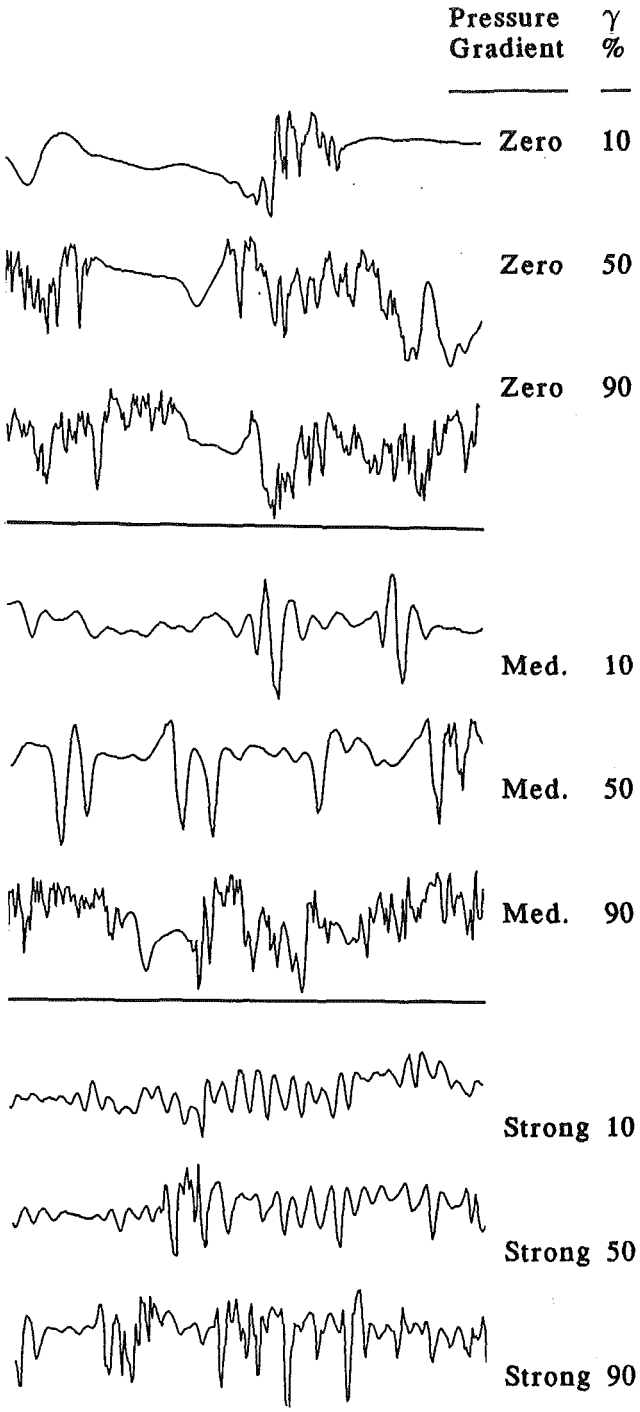

Fig. 6 Representative anemometer traces for three pressure gradients at three intermittency levels; each trace is of 40 ms duration

The high pressure gradient traces are marked by a fairly continuous appearance of instability waves, which show greater uniformity of amplitude than at the lower pressure gradients, although there is definite evidence of low-frequency amplitude modulation. The amplitude and frequency of the T-S waves under adverse pressure gradient conditions are higher than for lower pressure gradients and generally of the same order as the turbulent spots. Little information is available on turbulent spots under these conditions and especially on their spanwise structure. In essence though, whereas for weak adverse pressure gradients the T-S waves occur in packets, often associated with a single turbulent spot, for strong adverse pressure gradients the turbulent activity tends to be associated with each T-S wave. These observations are fully consistent with the observations of Knapp and Roache (1968), and are also in agreement with the study of Arnal et al. (1979a). As noted by Arnal et al., the more progressive way in which turbulence appears during transition in an adverse pressure gradient makes the turbulent spots much more difficult to characterize. Intermittency measurements are open to greater error in this case, and the high-pass filter setting of the intermittency meter requires particular care; too low a cutoff frequency will result in an erroneously early start of transition due to triggering from well-developed instability waves, while too high a setting will indicate a delayed transition onset due to the elimination of some genuine turbulent signals.

Velocity Fluctuation Spectra. To complement the hot-wire anemometer traces, spectra of longer samples, around 70 sec, were obtained using an HP3582A analyzer. The resulting distributions are presented in Figs. 7 and 8.

Figure 7 presents spectra plotted to identical scales (8 mv full scale) for a strong adverse pressure gradient (DP6). The intermittency level increases from 1 to 90 percent and a discrete frequency of 740 Hz, corresponding to the basic T-S wave, predominates throughout.

In Fig. 8, spectra are presented for an intermittency of 10 percent for the eight values of pressure gradient tested. The spectra for the low pressure gradient cases, DP0 and DP1, are presented with a different frequency scale from the others. Each square represents 250 Hz for DP0 and DP1 and 500 Hz for the remaining pressure gradients. A continuous change in spectral shape is observed as the streamwise pressure gradient becomes more adverse. In the absence of a pressure gradient, the spectral density falls continuously with increasing frequency and there are no identifiable spectral peaks. The application of a slight adverse pressure gradient produces a peak or peaks, which build in amplitude as the pressure gradient strengthens. For strong adverse pressure gradients, in which the laminar boundary layer is approaching separation, the spectra develop a plateau at low frequencies.

Table 1 compares the observed spectral peaks with the estimated frequencies of the basic T-S instability waves obtained from equation (9), which approximates the frequency for maximum amplification rate. This should underestimate the dominant T-S wave frequency, which generally lies close to the frequency of disturbances having received the maximum amplification ratio.

Assuming the observed peak closest to the theoretical value corresponds to the basic instability wave, it is seen that equation (9) predicts the T-S wave frequency to within 30 percent. However, the theoretical value is not always an underestimate as expected, exceeding the observed frequency for low pressure gradients. This is possibly explained by the observed transition inception shape factor, H_s, having fallen below the local equilibrium value for a steady laminar boundary layer due to shear stresses generated by nonlinear wave amplification processes and incipient turbulent mixing. The observed value of H is typically 0.2–0.3 below the steady laminar value at x_S and this yields a correspondingly lower R_δ^*. Using a value of $R_{\delta S}^*$ from a steady laminar boundary layer calculation in equation (9) could therefore be expected to produce closer agreement with observed frequencies at low pressure gradients and slightly greater underestimates in strong pressure gradient conditions, with a more general tendency for the theoretical value to be low.

In any case, the estimates of frequency obtained from equation (9) are acceptably close for the intended application of transition length modeling, and surprisingly good considering the approximations involved. Even the most soundly based estimates obtained by using small disturbance theory to compute the frequencies receiving maximum amplification ratio

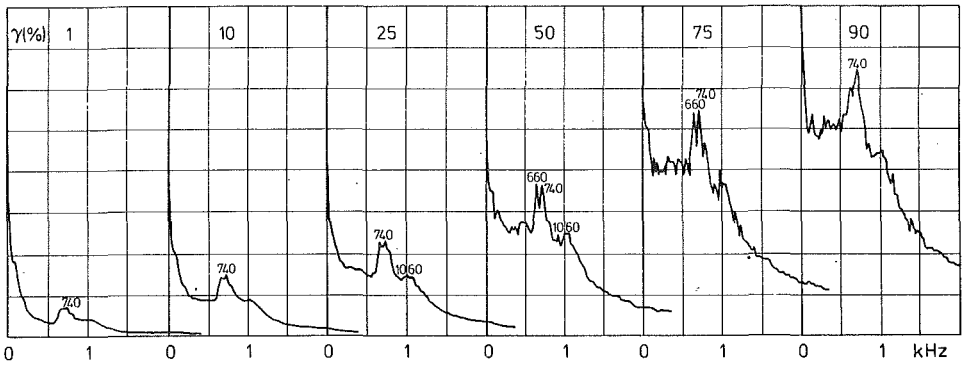

Fig. 7 Spectrum analyses for strong adverse pressure gradient and increasing intermittency levels

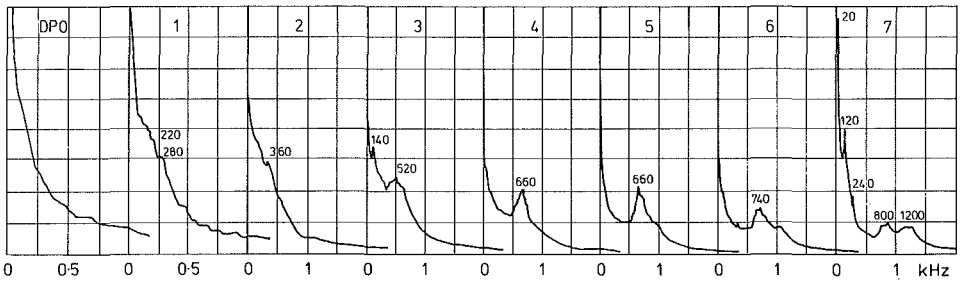

Fig. 8 Spectrum analyses at 10 percent intermittency for increasing levels of adverse pressure gradient

are only accurate to 10–20 percent (see, for example, Arnal et al., 1980).

The absence of a discrete peak in the spectrum for zero pressure gradient flow may appear anomalous in view of the order within wave sets, which can be identified in the hot-wire velocity traces for this case shown in Fig. 6. This can only be explained by a randomness in the frequency of appearance of wave sets, and in the frequency of waves within individual sets, over the long period of observation from which the spectrum was derived. Arnal et al. (1979a) obtained similar results.

For the mild adverse pressure gradient case, DP1, there is reasonable evidence for subharmonic behavior at half the frequency of a basic instability wave at 280 Hz. A distinct peak at 140 Hz was observed from other intermittency values. This tendency to exhibit subharmonics also is present in the spectra for DP2 and DP3. The work of Knapp and Roache (1968) indicated a greater tendency for the staggered type of vortex loop pattern to occur in zero pressure gradient flow during the nonlinear stage of laminar instability; this provides a possible explanation for the existence of subharmonics under mild pressure gradients.

For the moderate adverse pressure gradient cases, DP4 and DP5, only one spectral peak is observed. This is consistent with the spectrum for a single moderate pressure gradient case presented by Arnal et al. (1979a). For the strong pressure gradient cases, DP6 and DP7, a second spectral peak again become evident. In this case, the dominant frequencies are in the ratio 3:2, which can possibly be explained by a basic instability wave at the lower frequency combining with a subharmonic at half that frequency to produce the higher frequency peak. Although no clearly defined subharmonic peak is present in Fig. 8, other spectra show indications of a shoulder at half of the primary frequency. This behavior is reminiscent of that observed in separated laminar shear layers, e.g., Browand (1966). The subharmonic frequency in separated shear layers arises from a vortex-pairing phenomenon in which the cores of spanwise vortices produced by the basic instability processes rotate around each other. This is entirely different from the mechanism of vortex loop thatching, which gives rise to the subharmonic observed in near-zero pressure gradient flows.

Table 1 Comparison of observed and theoretical spectral peaks; observations correspond to 10 percent intermittency

Case	Observed Primary Peaks (Hz)	Theoretical T-S Wave Frequency (Hz)	Observed Secondary Peaks (Hz)
DP0	–	340	–
DP1	280	360	140, 220
DP2	360	470	–
DP3	520	510	140, 560
DP4	660	590	–
DP5	660	590	720
DP6	740	560	1060
DP7	800	610	120, 240, 1200

To summarize, the present results exhibit a continuous trend in behavior from spectra characteristic of zero pressure gradient to those typical of separated laminar shear layers. This suggests that it is not unreasonable to pursue the development of more generally applicable transition criteria embracing both separated and attached flows using $\lambda_{\theta t}$ as a parameter.

Comparison With Minimum Transition Length Model. A principal aim of the present investigation was to test the validity of the minimum transition length model proposed by Walker (1987). The data are presented in Fig. 9 in a new form that incorporates both pressure gradient and Reynolds number effects by plotting the ratio of observed transition length to that given by the minimum length model, equation (10), against the laminar pressure gradient parameter at transition inception, $\lambda_{\theta s}$. Figure 9 also includes the data of Gardiner (1987) and Arnal et al. (1979a), the only other known published results providing sufficient detail for this comparison.

The results of Sharma et al. (1982) are in general agreement with the present model although an accurate quantitative comparison is not possible and the free-stream turbulence level in that case was 2.4 percent. For Sharma's aft-loaded test configuration transition occurred in a moderate-to-strong adverse

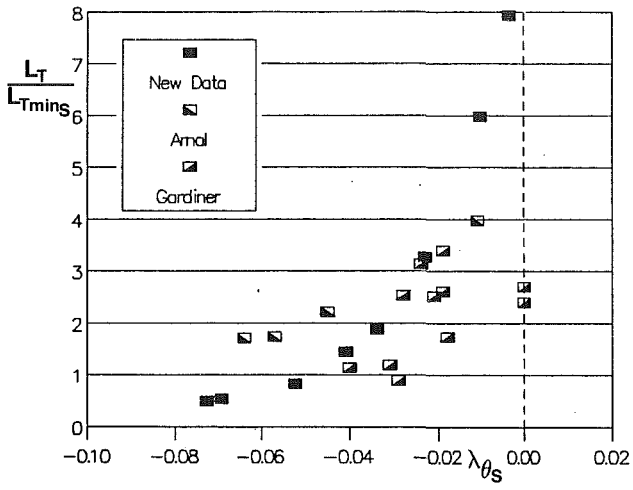

Fig. 9 Transition length data for transition inception at "S" compared with data of other authors

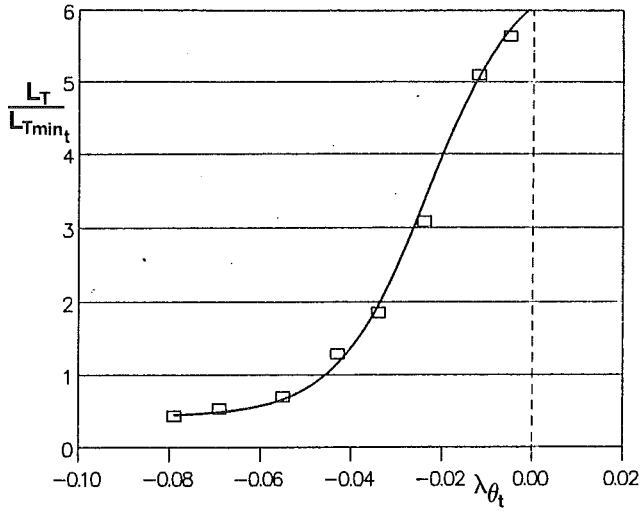

Fig. 10 Transition length data for transition inception at "t" fitted with new correlation curve, equation (13)

pressure gradient and the transition length was comparable with that predicted by equation (10). For Sharma's squared-off test configuration transition was initiated in a zero-to-mild adverse pressure gradient and the transitional flow length was about three times longer.

The data considered here all correspond to low turbulence flow situations. The present results were obtained with a free-stream turbulence level at inlet of 0.3 percent, while those of Arnal et al. were obtained with a turbulence level of 0.2 percent. Only the observations for turbulence levels of 0.3–0.4 percent have been included from the data of Gardiner.

In interpreting Fig. 9, it is important to appreciate that the limits of transitional flow in the data sets used were not all determined in exactly the same manner. Blair (1982) has previously commented on this problem and noted that transition lengths defined from velocity profile shape factor differed from those obtained from wall heat transfer data. The present results were obtained by intermittency measurement, with dimensionless velocity profile plots being used to confirm the establishment of fully turbulent flow. The present investigation, and that of Gardiner, used the 1 and 99 percent intermittency values to define the transition region. The published results of Arnal et al., however, define transition as starting when the shape factor H commences to decrease from its laminar value and finishing when H becomes essentially constant in the fully turbulent flow region. The lowest pressure gradient reading of Arnal et al. was obtained by extrapolation, necessitated by the extension of the transition region beyond the test surface.

Values of $L_T/L_{T\min}$ from the present investigation decrease monotonically with increasingly negative values of λ_{θ_S}. The data of Arnal et al. also show a rapid decrease but over a narrower range; the point obtained by extrapolation complicates interpretation of the Arnal results. Although the data of Gardiner are much more scattered, they also exhibit a tendency for $L_T/L_{T\min}$ to decrease as the pressure gradient becomes more adverse. The data envelope appears to approach a value of 1 ± 0.6, as the transitional laminar layer approaches separation.

The observed difference between the present results and those of Arnal et al. in strong adverse pressure gradients could be due to their definition of x_T, based on a stabilization of H, overestimating the transition length. The present results indicate that H is close to the local equilibrium turbulent flow value at the 99 percent intermittency point for the zero pressure gradient case, but increasingly exceeds this value as the pressure gradient becomes more adverse. This is consistent with the observation of Clauser (1954) that a turbulent boundary layer given a sudden perturbation may take a streamwise distance of 10 to 50 boundary layer thickness to regain equilibrium.

A transitional boundary layer is recovering from a laminar-type velocity profile with high H toward a fully turbulent profile with lower H and is in a similar situation to the perturbed turbulent layer. For the low pressure gradient data of Fig. 9, the transitional flow length is around 50–100δ giving adequate time for the equilibrium turbulent profile to be achieved when the intermittency reaches 99 percent. For the strongest adverse pressure gradient cases, however, the transition length decreases to 20–30δ and there is a distinct possibility that H may not have stabilized at the 99 percent intermittency point.

The data of Fig. 9 were presented on a basis of 1 percent intermittency for transition inception (the "S" basis) to provide a fair comparison with the data of other authors. Because the universal intermittency function of equation (1) provides a reasonable representation of the data for a wide range of pressure gradients, as demonstrated in Fig. 4, the use of the "t" basis for transition inception should give more consistent results. Accordingly the present data are plotted in this fashion in Fig. 10. The data have been presented in correlation form by fitting the curve

$$\frac{L_T}{L_{T\min}} = \frac{0.14 + 20\ \exp(100\lambda_{\theta t})}{0.33 + 3\ \exp(100\lambda_{\theta t})}. \tag{13}$$

This becomes asymptotic to 6.7 for favorable pressure gradients; the behavior in this regime needs to be confirmed experimentally.

Modeling Transition in an Adverse Pressure Gradient

The present investigation confirms the hypothesis of Walker (1987), which predicted a reduced transition length in decelerating flows, and the underlying physical explanation of this phenomenon. This is clearly seen from Fig. 10, which indicates about an order of magnitude reduction in transition length as the pressure gradient is increased from zero to the value producing incipient laminar separation.

This greatly reduced transition length in strong adverse pressure gradients is a fundamental prerequisite for the operation of an axial flow compressor, as indicated by Gostelow and Blunden (1988). Were the transition length not considerably shorter than indicated by flat plate correlations a turbulent boundary layer could not be developed on most compressor blades, which would consequently be incapable of sustaining the required loadings. The shorter transition lengths also are necessary for laminar separation bubbles to develop. If the

transition lengths were as great as those observed under zero pressure gradient conditions catastrophic laminar separation would be the normal flow regime.

The method of presenting transition length data for arbitrary pressure gradient by plotting $L_T/L_{T\min}$ against $\lambda_{\theta t}$ provides a universal approach to correlating transition length. It incorporates both Reynolds number (by way of $L_{T\min}$) and pressure gradient effects and also provides a rational basis for assessing existing transition criteria. The Narasimha (1978) correlation, equation (5), exhibits the same Reynolds number dependence as the minimum length model but makes no allowance for pressure gradient effects. The Chen and Thyson (1971) approach, which is basically an outgrowth of the Narasimha correlation, only allows for the influence of pressure gradient in respect of the secondary effect of changing free-stream velocity on turbulent spot convection rates; it makes no allowance for the primary influence of pressure gradient on the mechanics of instability and breakdown. On the other hand, attempts to allow for pressure gradient effects by seeking a correlation of $(R_{\theta_T} - R_{\theta_t})$ against $\lambda_{\theta t}$ do not admit any influence of transition inception Reynolds number on transition length.

With regard to the minimum transition length model, it is recalled that this was expected to apply for strong adverse pressure gradient conditions. Equation (13) indicates that the observed transition length essentially stabilizes around an $L_T/L_{T\min}$ value of 0.44 as laminar separation, corresponding to $\lambda_{\theta t}$ of -0.08, is approached. This is signficantly less than the transitional flow length ratio of unity corresponding to equation (10) and illustrates the necessity of calibrating the simple theoretical model against experimental data.

The development of the minimum transition length model incorporated the simplifying assumptions of the following:

(*a*) Breakdown occurring every cycle of the primary instability wave, at a frequency approximated by equation (9);
(*b*) The completion of transition at a streamwise position corresponding to the first longitudinal meeting of neighboring turbulent spots.

It is considered that the aforementioned assumptions (*a*) and (*b*) involve opposing errors, which cancel to some extent. On the one hand, the assumed spot inception frequency is mostly underestimated in strong adverse pressure gradients; this tends to increase the predicted value of $L_{T\min}$ by up to 30 percent. On the other hand, the development of turbulence in strong adverse pressure gradients may proceed more rapidly than indicated by the data, obtained from the spreading of isolated turbulent spots in a zero pressure gradient, used to formulate equation (10). This mechanism needs further investigation but its effect would be to decrease the predicted $L_{T\min}$.

In addition to the opposing errors, resulting from assumptions (*a*) and (*b*) previously mentioned, the present experimental results may underestimate transition length by up to 20 percent due to difficulties in measuring intermittency in strong adverse pressure gradients, which were not fully appreciated during the initial observations. This would justify a transition length under strong adverse pressure gradients rather closer to the theoretical value given by equation (10) than the present experimental data would appear to indicate.

In concluding, it is emphasized that the present investigation has deliberately focused on the effects of pressure gradient and avoided any extension to account for free-stream turbulence. Free-stream disturbances can be an important consideration in turbomachinery design and performance analysis. The authors, however, believe that a proper understanding of the mechanics of pressure gradient effects in isolation is an essential prerequisite for further studies of the combined influences of pressure gradient and free-stream disturbance on transitional flow.

Conclusions

Difficulties experienced by users of computational routines in calculating boundary layer development on the suction surfaces of airfoils and compressor blades, especially those operating at low Reynolds number, have highlighted the inadequacies of existing transition models. Transition length correlations developed from constant pressure flows will seriously overestimate the transition length in an adverse pressure gradient situation. A new and more universal correlation for transition under an adverse pressure gradient, incorporating both Reynolds number and pressure gradient effects, has been proposed and confirmed. The correlation applies to flows having a low free-stream turbulence level. Although two-dimensional viscous instability is the basic transition mechanism under these conditions for both zero and adverse pressure gradient flows, the physics of transition is rather different in the two cases. In the former case, transition occurs by breakdown of the laminar instability waves in sets, producing a random time-average disturbance spectrum. For an adverse pressure gradient, the Tollmien–Schlichting waves evolve more continuously and give a distinct spectral peak. The process is akin to forced transition and is accomplished in a much shorter streamwise distance.

In the absence of a streamwise pressure gradient, transition occurs relatively slowly and the new turbulent boundary layer essentially commences from a local equilibrium condition. For an adverse pressure gradient, on the other hand, the turbulent flow develops too quickly for the mean-flow boundary layer parameters to stabilize by the end of transition. The new turbulent layer may then be expected to commence with a higher form factor than that predicted by local equilibrium theory and transition lengths inferred from velocity profile data will be too high.

As the adverse pressure gradient becomes stronger, the unsteady flow component observed over a long time interval evolves continuously from random to periodic behavior. Significant subharmonic behavior at half the primary instability wave frequency is observed in very mild adverse pressure gradients (where it is believed to arise from vortex loop thatching) and in very strong adverse pressure gradients (where it may be associated with vortex pairing mechanisms typical of separated flow). The combination of subharmonic and primary wave may produce a spectral peak at a frequency 50 percent higher than that of the basic Tollmien–Schlichting wave.

The observed strong reduction in transition length under adverse pressure gradients, with the associated rapid increase in turbulent spot formation rate, is seen to be fundamental to the loading capability of an axial flow compressor. It is also an important factor in the formation of laminar separation bubbles, which significantly influence the low Reynolds number and off-design performance characteristics of turbomachinery blading. Further work is required to examine the combined effects of pressure gradients and free-stream disturbances.

Acknowledgments

The authors wish to acknowledge the careful experimentation of Mr. A. R. Blunden, at the University of Technology, Sydney. The University of Oxford has given valued support to the second author during a period of sabbatical leave. Appreciation also is expressed for the active encouragement of Dr. P. Stow, Mr. N. T. Birch, Mr. P. Clark and Mr. D. H. Brierley of Rolls-Royce plc.

References

Abu-Ghannam, B. J., and Shaw, R., 1980, "Natural Transition of Boundary Layers—The Effects of Turbulence, Pressure Gradient and Flow History," *Journal of Mechanical Engineering Science*, Vol. 22, No. 5, p. 213.

Alt, P., 1987, "An Intermittency Meter for Investigating Boundary Layer

Transition," University of Technology, Sydney, Technical Report NSWIT/ME 17.

Arnal, D., Juillen, J-C., and Michel, R., 1979a, "Analyse Experimentale de la Transition de la Couche Limite avec Gradient de Pression Nul ou Positif," ONERA T.P. No. 1979-8.

Arnal, D., and Juillen, J-C., 1979b, "Resultats Experimentaux Relatifs a l'Influence des Processus de Transition sur la Structure Initiale d'une Couche Limite Turbulente," AGARD CP-271, Turbulent Boundary Layers—Experiments, Theory and Modeling.

Arnal, D., Habiballah, M., and Delcourt, V., 1980, "Synthese sur les Methodes de Calcul de la Transition Developpees au D.E.R.A.T.," ONERA, CERT, Rapport Technique OA No. 11/5018.

Blair, M. F., 1982, "Influence of Free-Stream Turbulence on Boundary-Layer Transition in Favorable Pressure Gradients," ASME *Journal of Engineering for Power*, Vol. 104, pp. 743-750.

Browand, F. K., 1966, "An Experimental Investigation of the Instability of an Incompressible, Separated Shear Layer," *Journal of Fluid Mechanics*, Vol. 26, pp. 281-307.

Cebeci, T., and Smith, A. M. O., 1974, *Analysis of Turbulent Boundary Layers*, Academic Press, New York.

Chen, K. K., and Thyson, N. A., 1971, "Extension of Emmons' Spot Theory to Blunt Bodies," *AIAA Journal*, Vol. 9, pp. 821-825.

Clauser, F. H., 1956, "The Turbulent Boundary Layer," *Advances in Applied Mechanics*, Vol. IV, pp. 1-51.

Craik, A. D. D., 1971, "Nonlinear Resonant Instability in Boundary Layers," *Journal of Fluid Mechanics*, Vol. 50, pp. 393-413.

Dhawan, S., and Narasimha, R., 1958, "Some Properties of Boundary Layer Flow During the Transition From Laminar to Turbulent Motion," *Journal of Fluid Mechanics*, Vol. 3, pp. 418-436.

Emmons, H. W., 1951, "The Laminar-Turbulent Transition in a Boundary Layer—Part I," *Journal of Aeronautical Sciences*, Vol. 8, pp. 490-498.

Gardiner, I. D., 1987, "Transition in Boundary Layer Flows," PhD Thesis, College of Technology, Dundee, Scotland.

Gostelow, J. P., and Blunden, A. R., 1988, "Investigations of Boundary Layer Transition in an Adverse Pressure Gradient," ASME Paper No. 88-GT-298.

Gostelow, J. P., Blunden, A. R., and Blunden, W. R., 1988, "Measurements and Stochastic Analysis of Boundary Layer Transition for a Range of Free-Stream Turbulence Levels," *Proceedings 2nd International Symposium on Transport Phenomena, Dynamics and Design of Rotating Machinery*, Honolulu, HI.

Herbert, T., 1983, "Modes of Secondary Instability in Plane Poiseuille Flow," *Proceedings IUTAM Symposium on Turbulence and Chaotic Phenomena in Fluids*, Kyoto, Japan.

Kegelman, J. T., and Mueller, T. J., 1986, "Experimental Studies of Spontaneous and Forced Transition on an Axisymmetric Body," *AIAA Journal*, Vol 24, pp. 397-403.

Klebanoff, P. S., Tidstrom, K. D., and Sargent, L. H., 1962, "The Three-Dimensional Nature of Boundary Layer Instability," *Journal of Fluid Mechanics*, Vol. 12, pp. 1-34.

Knapp, C. F., and Roache, P. J., 1968, "A Combined Visual and Hot-Wire Anemometer Investigation of Boundary Layer Transition," *AIAA Journal*, Vol. 6, pp. 29-36.

McCormick, M. E., 1968, "An Analysis of the Formation of Turbulent Patches in the Transition Boundary Layer," ASME *Journal of Applied Mechanics*, Vol. 35, pp. 216-219.

Narasimha, R., 1957, "On the Distribution of Intermittency in the Transition Region of a Boundary Layer," *Journal of Aero. Science*, Vol. 24, pp. 711-712.

Narasimha, R., 1978, "A Note on Certain Turbulent Spot and Burst Frequencies," Report 78FM10, Dept. Aero. Eng., Indian Institute of Science.

Narasimha, R., 1985, "The Laminar-Turbulent Transition Zone in the Boundary Layer," *Prog. in Aerospace Sci.*, Vol. 22, pp. 29-80.

Obremski, H. J., Morkovin, M. V., and Landahl, M., 1969, "A Portfolio of Stability Characteristics of Incompressible Boundary Layers," AGARDograph 134.

Saric, W. S., and Thomas, A. S. W., 1983, "Experiments on the Subharmonic Route to Turbulence in Boundary Layers," *Proceedings IUTAM Symposium on Turbulence and Chaotic Phenomena in Fluids*, Kyoto, Japan.

Schubauer, G. B., and Klebanoff, P. S., 1956, "Contributions on the Mechanism of Boundary Layer Transition," NACA Report 1289.

Schubauer, G. B., and Skramstad, H. K., 1948, "Laminar Boundary Layer Oscillations and Transition on a Flat Plate," NACA Report 909.

Sharma, O. P., Wells, R. A., Schlinker, R. H., and Bailey, D. A., 1982, "Boundary Layer Development on Turbine Airfoil Suction Surfaces," ASME *Journal of Engineering for Power*, Vol. 104, pp. 698-706.

Subroto, P. H., 1987, "Viscous/Inviscid Interaction Analysis of the Aerodynamic Performance of the NACA 65-213 Airfoil," Master's Thesis, Naval Postgraduate School, Monterey, CA.

Walker, G. J., 1987, "Transitional Flow on Axial Turbomachine Blading," AIAA Paper No. 87-0010.

Walker, G. J., Subroto, P. H., and Platzer, M. F., 1988, "Transition Modeling Effects on Viscous/Inviscid Interaction Analysis of Low Reynolds Number Airfoil Flows Involving Laminar Separation Bubbles," ASME Paper No. 88-GT-32.